Two-step mineralization of Tartrazine solutions: Study of parameters and by-products during the coupling of electrocoagulation with electrochemical advanced oxidation processes

CrossMark

Abdoulaye Thiam [a,b], Minghua Zhou [a,*], Enric Brillas [b], Ignasi Sirés [a,b,*]

[a] College of Environmental Science and Engineering, Nankai University, Tianjin 300071, China
[b] Laboratori d'Electroquímica dels Materials i del Medi Ambient, Departament de Química Física, Facultat de Química, Universitat de Barcelona, Martí i Franquès 1-11, 08028 Barcelona, Spain

ABSTRACT

A novel sequential electrochemical treatment consisting in an electrocoagulation (EC) pre-treatment and the subsequent advanced oxidation by photoelectro-Fenton (PEF) process with in-situ H_2O_2 electrogeneration and UVA light irradiation has been envisaged for the removal of organic pollutants from water, showing a high performance for the decolorization and mineralization of Tartrazine (Acid Yellow 23) solutions. EC has a dual purpose as a coagulation and catalyst source step since it allows the formation of $Fe(OH)_n$ ($n = 2$ or 3) coagulant and Fe^{3+}/Fe^{2+} ions. The influence of the anode material (Fe and Al), supporting electrolyte, pH and current during the individual EC on the abatement of color and total organic carbon (TOC) has been assessed. EC with Fe in 0.05 M NaCl yielded the best results. Next, various single electrochemical advanced oxidation processes (EAOPs) such as electro-oxidation (EO), electro-Fenton (EF) and PEF with a Pt or boron-doped diamond (BDD) anode and an air-diffusion cathode (ADE) have been tested. PEF with BDD/ADE yielded the quickest degradation among all the EAOPs in NaCl, due to the action of oxidants like active chlorine as well as $^{\bullet}OH$ formed at the anode surface from H_2O oxidation and in the bulk from UV-enhanced Fenton's reaction between cathodic H_2O_2 and added Fe^{2+}. Therefore, the two-step EC (Fe/steel)/PEF (BDD/ADE) process was the best EC/EAOP combination. The EC treatment in 0.05 M NaCl at natural pH 6.3 and 200 mA, followed by PEF treatment of the supernatant at pH 3.0 and 200 mA, yielded the best conditions with a total decolorization in 15 min of EC and total mineralization in ca. 300 min of PEF. GC–MS analysis showed the formation of several benzenic by-products during the application of EC/PEF. Independent electrolyses revealed the ability of EC to accumulate soluble chlorobenzene derivatives, which can be completely destroyed in the PEF step under the action of the mixture of oxidants, particularly by successive hydroxylation via $^{\bullet}OH$ largely promoted in the bulk by the Fe^{2+} ions generated in EC.

1. Introduction

Wastewaters generated by several industries pose some serious health and environmental risks worldwide owe to the significant concentrations and/or large variety of toxic aromatic pollutants. In this context, the advanced oxidation processes (AOPs) are very effective remediation technologies due to the action of highly reactive species (ROS) such as (mainly but not uniquely) hydroxyl radical ($^{\bullet}OH$) in the reaction mechanism. The main catalyzed AOPs can be divided into: (i) heterogeneous catalysis such as TiO_2 photocatalysis and electrocatalysis (EAOPs) with large O_2-overvoltage anodes, and (ii) homogeneous catalysis such as catalyzed ozonation and chemical and electrochemical Fenton and photo-Fenton [1–3].
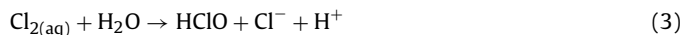
In recent years, the interest on new or enhanced electrochemical separation and degradation technologies has grown considerably. Most intensive research efforts are devoted to heterogeneous electrocatalysis, where electro-oxidation (EO) is predominant, electrocoagulation (EC) and EAOPs based on Fenton's reaction chemistry [4–6]. EO combines high simplicity and efficacy, favoring the oxidative decontamination of waters under the action of $^{\bullet}OH$ formed at the anode surface by water oxidation via reaction (1). At present, boron-doped diamond (BDD) is the best electrocatalytic anode material to oxidize pollutants, which has led to the

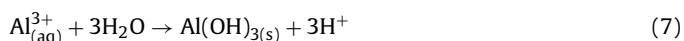* Corresponding authors. Tel.: +34 934021223/+86 2266229619; fax: +34 934021231/+86 2223501117.

E-mail addresses: zhoumh@nankai.edu.cn (M. Zhou), i.sires@ub.edu, isiresa@gmail.com (I. Sirés).

development of successful flow reactors [7–10]. In chloride medium, the oxidation mediated by active chlorine species (Cl_2, $HClO$ and/or ClO^-) electrogenerated via reactions (2)–(4) competes with the $^\bullet OH$-mediated oxidation [6].

$$M + H_2O \rightarrow M(^\bullet OH) + H^+ + e^- \quad (1)$$

$$2Cl^- \rightarrow Cl_{2(aq)} + 2e^- \quad (2)$$

$$Cl_{2(aq)} + H_2O \rightarrow HClO + Cl^- + H^+ \quad (3)$$

$$HClO \rightleftarrows ClO^- + H^+ \quad (4)$$

EC is a traditional physicochemical treatment for phase separation that is based on the release of Al(III) or Fe(II) cations in the bulk from dissolution of the corresponding sacrificial anode(s) via reactions (5) and (6). These are active coagulant precursors because the simultaneous production of OH^- anions by cathodic reduction of water leads to the formation of insoluble polymeric metallic hydroxides as shown in reactions (7) and (8). Such particles have large surface area and remain as a gelatinous suspension, then being able to remove pollutants by coagulation upon destabilization either by surface complexation or electrostatic attraction [11–13]. EC has been shown effective for the removal of colloidal and ionic pollutants from synthetic and real waters [14–22].

$$Al_{(s)} \rightarrow Al^{3+}_{(aq)} + 3e^- \quad (5)$$

$$Fe_{(s)} \rightarrow Fe^{2+}_{(aq)} + 2e^- \quad (6)$$

$$Al^{3+}_{(aq)} + 3H_2O \rightarrow Al(OH)_{3(s)} + 3H^+ \quad (7)$$

$$4Fe^{2+}_{(aq)} + 10H_2O + O_{2(g)} \rightarrow 4Fe(OH)_{3(s)} + 8H^+_{(aq)} \quad (8)$$

EAOPs such as electro-Fenton (EF) and photoelectro-Fenton (PEF) processes are even more efficient than EO and EC for the destruction of aqueous pollutants [23–36]. They are based on the in-situ electrogeneration of H_2O_2 into acidic polluted solutions from the two-electron O_2 reduction at a carbonaceous cathode. The addition of a catalytic amount (0.1–1.0 mM) of Fe^{2+} to the medium allows a high production of $^\bullet OH$ in the solution bulk from the well-known Fenton' reaction [5]:

$$Fe^{2+} + H_2O_2 \rightarrow Fe^{3+} + {}^\bullet OH + OH^- \quad (9)$$

PEF has the greatest performance owing to the concomitant action of both the generated $^\bullet OH$ and the UV radiation on the organic molecules and their Fe(III)-complexes [30,33,35]. Although EF and PEF are promising technologies, their potential exploitation is still limited due to the relatively high operation costs that are inherent to the long treatment time required. Aiming to shorten the reaction time, the so-called peroxi-coagulation (PC) process with a sacrificial iron anode and a cathode able to generate H_2O_2 has been further devised [37–39]. This one-pot method allows the simultaneous coagulation and oxidation of organic pollutants thanks to Fe^{2+} catalyst generated on site via reaction (6), but it presents some major drawbacks: (i) The excess of iron cations causes the destruction of $^\bullet OH$, (ii) the cathode lifetime and its ability for producing H_2O_2 are drastically reduced due to both, adsorption of coagulated particles that block the diffusion pores and the active sites, and surface abrasion caused by precipitated hydroxides and coagulated matter, and (iii) the effect of UV light in photoperoxi-coagulation is almost negligible due to the barrier effect of the iron precipitate.

Synthetic dyes are being largely produced due to their unique properties that allow limitless industrial applications. Azo dyes are particularly pre-eminent since they represent 60–70% of the world production [18]. However, their occurrence in wastewaters entails major concerns due to the proven toxicity and carcinogenicity and the production of toxic by-products like aromatic amines [31,40]. Among them, food azo-colors have received much less attention than their textile counterparts, despite being considered dangerous due to their possible connection to hyperactivity in children in cases of intakes of potent mixes of colorings. Recent issues over the toxicity of food additives have led to a stricter legislation. For example, the UK Foods Standards Agency has recommended that they should be phased out over a period from food and drink in the EU [41]. Tartrazine (Acid Yellow 23, trisodium 1-(4-sulfonatophenyl)-4-(4-sulfonatophenylazo)-5-pyrazolone-3-carboxylate) is primarily used as a common synthetic food coloring agent, also known as additive E102, to provide a vivid yellow color to processed commercial foods like sweets, beverages and snacks. It is also used in personal care and cosmetic products, as well as in medications. Sensitivity to Tartrazine may be relevant since it is suspected to be responsible for most of the allergic and intolerance reactions among all azo dyes, even being temporally banned in some European countries. Its adverse reactions in human beings have lately been under consideration by the European Food Safety Agency [42]. A large range of dyestuffs has been removed from water electrochemically by EO [8,9,17,43,44], EC [14,17,19,21] and EAOPs like EF and PEF [23–26,31,33,45,46]. However, there are no studies assessing the performance of BDD or PEF for Tartrazine, and just a couple of studies report its treatment by EC [47,48].

As far as we know, this work reports for the first time the sequential combination of EC and EAOPs based on Fenton's reaction chemistry, aiming at: (i) inducing the coagulation of a large amount of organic matter via the EC pre-treatment, which also acts as a source of iron catalyst, and (ii) controlling the electrogeneration of oxidizing agents on site to reach the complete mineralization of dye solutions during the EAOP post-treatment. This intends to overcome the drawbacks exposed for PC, therefore achieving a higher degradation performance for dye solutions. Previous EC/EAOPs couplings reported in literature for decontamination have dealt with the EC/EO system [49–51]. The present study focuses on the treatment of solutions of 130 ml of Tartrazine as a model food azo dye in different electrolytes at constant current. First, the individual EC with Fe or Al anodes, and EO, EF and PEF with Pt or BDD anodes were tested to assess the effect of the experimental parameters on the decolorization and TOC removal rates. Then, the best combined EC/EAOP was optimized to achieve the quickest decontamination. The degradation by-products formed during this combined treatment were identified by gas chromatography coupled to mass spectrometry (GC–MS).

2. Experimental

2.1. Chemicals

Tartrazine ($C_{16}H_9N_4Na_3O_9S_2$, C.I. 19140, dye content $\geq$85%) was purchased from Sigma-Aldrich and was used as received. Anhydrous sodium sulfate, sodium chloride and sodium nitrate used as background electrolytes, as well as iron(II) sulfate heptahydrate, used as catalyst in EF and PEF, were of analytical grade from Merck and Fluka. Solutions were prepared with ultra-pure water from a Millipore Milli-Q system with resistivity >18 MΩ cm and their pH was adjusted with analytical grade sodium hydroxide or sulfuric, hydrochloric or nitric acid from Merck. Other chemicals for performing analyses were obtained from Merck and Sigma-Aldrich.

2.2. Electrochemical cells

All the electrolytic trials were conducted in an open and undivided cylindrical glass cell of 150 ml capacity with a double jacket

for circulation of external thermostated water to regulate the solution temperature at 25 °C.

For the EC trials, the anode was either an iron or aluminium plate with overall dimensions of 5.0 cm × 1.5 cm, 0.25 cm thickness, and immersed length of 3.0 cm. The cathode was a steel plate with the aforementioned dimensions. The front, back and sides of each piece were exposed to the solution. The electrodes were placed in parallel with an interelectrode gap of 1.0 cm. Before first use, all electrodes were mechanically abraded using SiC paper to remove scale, followed by cleaning with 0.1 M NaOH or H_2SO_4 solution (20% in volume) and a final ultrasonic cleaning in ultra-pure water.

For the EAOPs, the anode was either a 3 cm^2 Pt sheet of 99.99% purity supplied by SEMPSA (Barcelona, Spain) or a 3 cm^2 BDD thin-film electrode supplied by NeoCoat (La-Chaux-de-Fonds, Switzerland). The latter one was synthesized by the HFCVD technique on p-type polycrystalline Si wafers (0.1 Ω cm, Siltronix), being the BDD coating 2.5–3.5 μm thick and having 700 ppm of boron. The cathode was either a 3 cm^2 stainless steel plate or a 3 cm^2 carbon-PTFE air-diffusion electrode (ADE) supplied by E-TEK (Somerset, NJ, USA), mounted as described elsewhere and fed with air pumped at 1 l min^{-1} for continuous H_2O_2 generation [5]. The interelectrode gap was about 1.0 cm. Before first use, a preliminary polarization in 100 ml of 0.05 M Na_2SO_4 at 100 mA cm^{-2} for 180 min allowed the removal of the impurities of the BDD anode surface and the activation of the ADE. PEF treatments were carried out under irradiation with a Philips TL/6W/08 fluorescent black light blue tube that was placed at 7 cm above the solution. This tube emitted UVA light in the wavelength region 320–400 nm with λ_{max} = 360 nm, yielding a photoionization energy of 5 W m^{-2} as detected with a Kipp & Zonen CUV 5 radiometer.

Freshly prepared solutions of 130 ml with 100 mg l^{-1} of TOC (corresponding to 278 mg l^{-1} or 0.52 mM) of Tartrazine in different supporting electrolytes (Na_2SO_4, NaCl or $NaNO_3$) were treated by individual EC and EAOPs. In EC, the effect of the applied current was tested in the range 50–300 mA and the solution pH was varied between 3.0 and 11, whereas it was fixed at 3.0 in trials of EAOPs because this pH has been found as optimal for the treatment of other aromatics with ADE as cathode [5]. In EF and PEF, 0.5 mM Fe^{2+} was added as catalyst. To perform the combined EC/EAOPs, EC-treated solutions were centrifuged for 5 min at 5000 rpm in order to remove the precipitate and easily collect the supernatant to be further treated by each EAOP. The solutions were always vigorously stirred with a magnetic bar at 800 rpm to ensure mixing and the transport of reactants toward/from the electrodes.

2.3. Apparatus and analysis procedures

All the experiments were performed at constant current with an Amel 2053 potentiostat-galvanostat, which also displayed the potential difference between electrodes. The solution pH was measured with a Crison 2000 pH-meter. Samples were always withdrawn at regular time intervals from the treated solutions and then microfiltered with 0.45 μm PTFE filters from Whatman before analysis. The decolorization of Tartrazine solutions was monitored from the absorbance (A) decay at the maximum visible wavelength (λ_{max}) of 428 nm, measured from the spectra recorded on a Shimadzu 1800 UV/Vis spectrophotometer at 35 °C. The percentage of color removal or decolorization efficiency was then determined according to Eq. (10) [5,18]:

$$\text{Color removal } (\%) = 100 \frac{A_0 - A_t}{A_0} \tag{10}$$

where A_0 and A_t denote the absorbance at initial time and after an electrolysis time t, respectively.

The same spectrophotometer was also employed for colorimetric measurements of free active chlorine (Cl_2 and HClO/ClO$^-$) and

total iron concentrations. Active chlorine was determined by the DPD method, which consists in the reaction between the desired sample and a standard *N,N*-diethyl-*p*-phenylenediamine (DPD) solution to generate a pink color measured at λ = 515 nm whose intensity is proportional to the active chlorine content [52]. The total iron content was obtained by adding ascorbic acid to selected samples and measuring the light absorption of the complex formed between Fe^{2+} and 1,10-phenanthroline at λ = 508 nm [53]. The mineralization of solutions was monitored from the decay of their TOC determined on a Multi N/C® 3100 analyzer from Analytik Jena. Reproducible TOC values with an accuracy of ±1% were always found by injecting 50 μl aliquots into the analyzer. The energy consumption per unit volume was then calculated as follows [5]:

$$\text{Energy consumption } \left(\text{kW h m}^{-3} \right) = \frac{E_{cell} It}{V_s} \tag{11}$$

where E_{cell} is the average potential difference between electrodes (V), I is the applied current (A), t is the electrolysis time (h) and V_s is the volume of the treated solution (l).

The aromatic by-products in some treated solutions were identified by GC–MS using an Agilent Technologies system composed of a 7890A gas chromatograph equipped with a 7683B series injector and a 5975C mass spectrometer in EI mode at 70 eV. A nonpolar Agilent J&W HP-5ms column with dimensions of 0.25 μm, 30 m × 0.25 mm (i.d.) was used. The temperature ramp was as follows: 36 °C for 1 min, 5 °C min^{-1} up to 300 °C and hold time 10 min. The temperature of the inlet, source and transfer line was 250, 230 and 280 °C, respectively. The analyses were by splitless (0.7 min) injection. Aiming to identify as many reaction intermediates as possible, the organic components of the whole electrolyzed volumes (i.e., 130 ml) in each trial were extracted with CH_2Cl_2 in three times of 25 ml each. The resulting organic solution was dried over anhydrous Na_2SO_4, filtered and concentrated up to ca. 1 ml under reduced pressure to be further analyzed. The mass spectra were identified with a NIST05 MS library.

3. Results and discussion

3.1. Treatment of Tartrazine solutions by electrocoagulation alone

The effect of several experimental parameters on the decolorization and decontamination profiles obtained during the treatment of 278 mg l^{-1} Tartrazine by EC was firstly assessed with Fe/steel as the anode/cathode pair. Different electrolyses were performed in 0.05 M Na_2SO_4, NaCl or $NaNO_3$ at 300 mA in order to study the influence of the type of supporting electrolyte. All these trials were conducted at natural pH 6.3, which was under continuous control because it tended to increase due to the generation of OH$^-$ at the cathode that could be only partially neutralized by H$^+$ formed from reaction (8) [54]. The decolorization efficiency is represented in Fig. 1a as the increasing percentage of color removal at 428 nm over the electrolysis time. The absorption spectrum of Tartrazine is included in the inset, showing an absorption band in the UV region at about 254 nm corresponding to the benzenic rings and a broader band in the visible region at 428 nm related to the –N=N– bond that is responsible for the vivid lemon yellow color. In Na_2SO_4, the intensity of both absorption bands decreased continuously and rapidly, reaching the total disappearance of the band at 428 nm in 30 min. This can be explained by the iron dissolution via reaction (6) to yield Fe^{2+}, which is further transformed into a powerful coagulant like Fe(OH)$_n$ with n = 2 or 3 at pH > 1.0. The decolorization rate was even faster in NaCl, the solution becoming colorless after only 10 min. In this case, coagulation by Fe(OH)$_n$ species coexists with oxidation mediated by active chlorine, which may be formed by anodic discharge of chloride anions as shown in reactions (2)–(4). The formation of soluble (FeCl)$_n$ complexes can
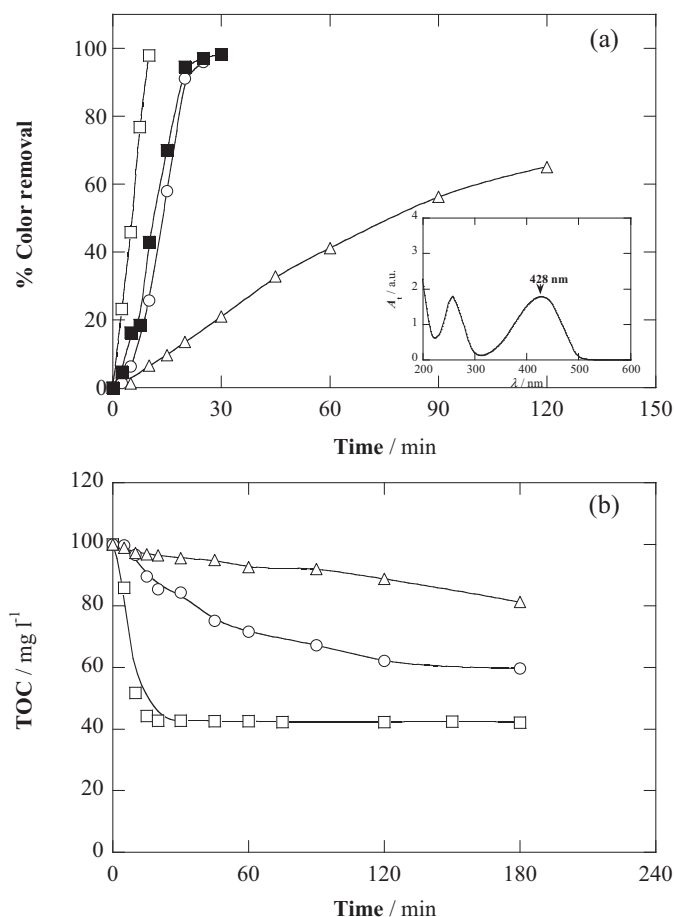
Fig. 1. Effect of the type of supporting electrolyte on the (a) decolorization efficiency at 428 nm and (b) TOC removal with electrolysis time for the EC (Fe/steel) degradation of 130 ml of 278 mg l^{-1} Tartrazine solutions in 0.05 M ($\bigcirc$) Na$_2$SO$_4$, ($\square$) NaCl, and ($\triangle$) NaNO$_3$, at natural (and controlled) pH 6.3 and 300 mA. In (a), ($\blacksquare$) comparative color removal obtained with the EC (Al/steel) treatment in 0.05 M NaCl. The inset panel in plot (a) shows the absorption spectrum for the initial Tartrazine solution.

also contribute to the enhanced removal because this allows the increase of the soluble iron dose. Note that a careful analysis of the UV/Vis spectra in Na$_2$SO$_4$ and NaCl media revealed the presence of residual absorbance at 254 nm even once the absorbance at 428 nm became zero. In contrast, protracted electrolyses in NaNO$_3$ showed a much slower decrease of the absorbance, reaching only 65% of color removal at 120 min. Recent studies have proven that the dissolution of sacrificial Fe is hindered by nitrate salts, therefore yielding very low degradation efficiencies because flocs cannot be formed as required [20,55]. This was corroborated here by means of anode weighting before and after the electrolyses, which showed that the current efficiency for iron dissolution was as low as 0.1% in NaNO$_3$ and around 100% in Na$_2$SO$_4$ and NaCl.

Fig. 1a also shows the comparative EC treatment in 0.05 M NaCl using Al as the anode because it is a widely used material in this technique. The color totally disappeared after just 30 min, which represents a high removal rate. In the case of Al, however, the addition of chloride inhibits or slows down the anode passivation, which is a typical phenomenon for Al in other media due to the formation of an isolating, compact oxide interlayer. But, the progress of the color removal was significantly slower than that obtained with the Fe anode, as also occurred in other works on EC [48]. In fact, at 10 min, only 43% decolorization was achieved with Al instead of 100% reached with Fe. Since the formation of Al(OH)$_3$ through consecutive reactions (5) and (7) accounts for the coagulation of the organic matter, the different performance of both

anodes can be plausibly explained by: (i) their different ability to promote charge neutralization, and (ii) the lower adsorption ability of Al(OH)$_3$ compared to Fe(OH)$_n$, which complicates the sweep flocculation mechanism to entrap the colloidal matter. Iron anodes were then preferred, not only due to the enhanced coagulation but also to the superior catalytic properties of Fe^{2+} if thinking in a later coupling with Fenton-based EAOPs.

Fig. 1b depicts the TOC removal profiles obtained during the EC (Fe/steel) experiments shown in Fig. 1a. The efficacy for removing the organic matter was greatly dependent on the electrolyte, thus increasing in the order NaNO$_3$ < Na$_2$SO$_4$ < NaCl in accordance with the decolorization efficiency discussed above. However, it can be seen that none of the systems allowed the complete decontamination of the solutions. In NaCl medium, the synergistic action of coagulation by Fe(OH)$_n$ and oxidation by active chlorine only yielded 60% TOC abatement at about 10 min, thereby remaining constant over time. This can therefore be justified by the accumulation of persistent organic by-products that contribute to the remaining TOC, which agrees perfectly with the previous comments about the residual UV absorbance observed at 254 nm once reached the total decolorization at 10 min. It can then be inferred that the residual TOC corresponds to colorless aromatic by-products, as later confirmed by GC–MS results.

Since EC (Fe/steel) in NaCl yielded the best results, all the subsequent EC experiments were performed in this medium. First, the effect of the electrolyte concentration was studied in the range 0.025–0.3 M NaCl under the same experimental conditions of Fig. 1a, the potential difference between anode and cathode decreasing from 11.5 to 3.2 V as the chloride content increased. As can be seen in Fig. 2a, a higher NaCl concentration did not bring about any significant acceleration of the color removal and all the solutions were completely decolorized after 10–12 min. This means that the low chloride contents are already able to yield enough active chlorine so as to promote the maximum oxidation of Tartrazine in such a short time period. On the other hand, the NaCl concentration had a slightly higher effect on TOC removal. As shown in Fig. 2b, the decontamination rate increased from 0.025 to 0.05 M NaCl, and then progressively decreased as the NaCl content was raised up to 0.3 M, always achieving the maximum TOC removal of 60%. This means that once reached a threshold amount of active chlorine already at low chloride contents, the additional benefits that could arise at higher chloride contents from a greater oxidative degradation are counteracted by the lower coagulation efficiency due to (i) the formation of persistent by-products that are harder to coagulate and (ii) the increased ionic strength that affects the equilibria of reactions between charged and/or colloidal species in EC.

It is known that the EC process is usually highly dependent on the solution pH due to the large range of equilibria involved. Fig. 3a depicts the time course of the decolorization efficiency for solutions of pH 3.0, 6.3 (natural pH), 9.0 and 11.0 treated in 0.05 M NaCl at 300 mA. The control of pH was necessary for trials at pH 3.0 and 6.3 because it tended to become more alkaline. As can be seen in the figure, the quickest color removal was achieved in 10 min at pH 6.3–11, whereas the process was quite slower at pH 3.0 with total color disappearance at 25 min. The explanation of this finding is that the Fe(OH)$_2$ and Fe(OH)$_3$ flocs are more poorly produced at pH < 6.0 because of the neutralization of cathodically formed OH$^-$ by H$^+$ present in the medium and hence, the soluble Fe(II) and Fe(III) species show a certain stability that results in a slower decolorization, despite the fact that HClO with pKa = 7.55 is the dominant active chlorine species over the less oxidizing ClO$^-$ [18]. Fig. 3b shows the TOC decay during the same trials. The quickest decontamination was achieved at intermediate pH values of 6.3 and 9.0, due to the combination of coagulation with electrochlorination that yielded 60% TOC removal in both cases. In contrast, a slower and
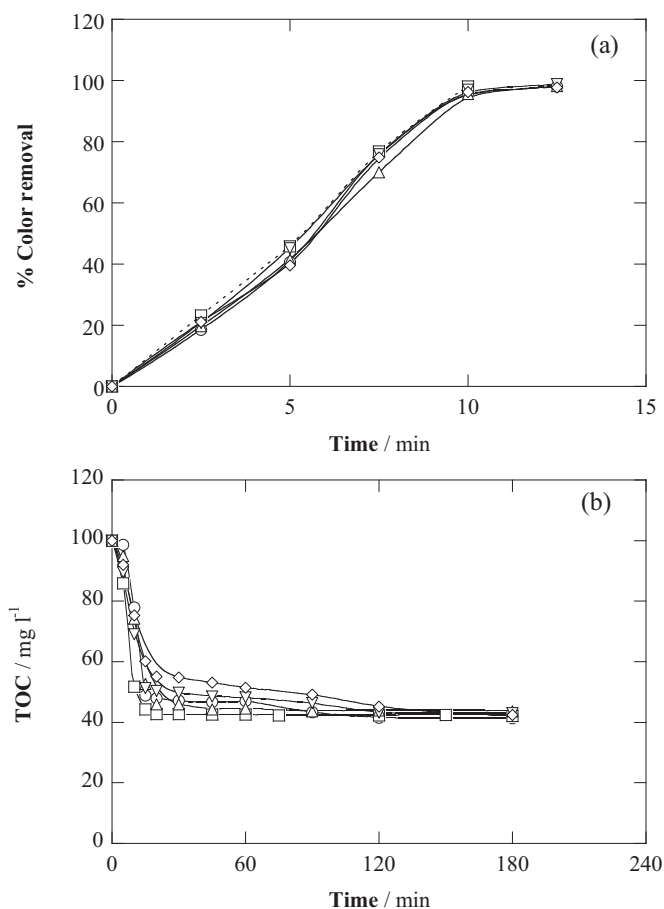
Fig. 2. Effect of the supporting electrolyte concentration on the (a) percentage of color removal at 428 nm and (b) TOC abatement with electrolysis time for the EC (Fe/steel) degradation of 130 ml of 278 mg l^{-1} Tartrazine solutions in: (○) 0.025 M, (□) 0.05 M, (△) 0.1 M, (▽) 0.15 M and (◇) 0.3 M NaCl, at natural (and controlled) pH 6.3 and 300 mA.

Fig. 3. Effect of pH on the (a) decolorization efficiency at 428 nm and (b) TOC removal with electrolysis time for the EC (Fe/steel) degradation of 130 ml of 278 mg l^{-1} Tartrazine solutions in 0.05 M NaCl, at pH: (○) 3.0, (□) 6.3 (natural), (△) 9.0 and (▽) 11.0, all at 300 mA.

poorer TOC abatement was achieved at more acidic and alkaline pH, which can be mainly accounted for by the less favorable formation of Fe(OH)$_3$ coagulant according to the iron speciation diagrams. The TOC removal at 180 min was slightly greater at pH 11.0 compared to pH 3.0 due to the action of the more oxidizing ClO$^-$. Therefore, since the natural pH of Tartrazine solutions is 6.3, all the subsequent EC experiments were carried out at this pH, which increases the economic viability of the treatment.

The last key parameter studied for EC (Fe/steel) alone was the applied current, which was tested in the range 50–300 mA, resulting in average potential difference between electrodes increasing from of 2.7 to 10.2 V. Current not only determines the coagulant dosage rate, but also the bubble production rate and size, and all these factors eventually affect the EC efficiency [22]. According to Faraday's law, the dissolution of anode increases at higher current, thus producing more ions and hence, more flocs that trap the dye and its by-products. Furthermore, in NaCl medium the applied current has also great influence on the electrogeneration rate of Cl$_2$ that is further converted into HClO/ClO$^-$ in the bulk. According to Fig. 4a, the percentage of color removal was always 100%, but it was progressively faster when current was raised, thus shortening the process from 60 to 10 min when increasing from 50 to 300 mA. Such dependence with current is also evident in Fig. 4b for TOC abatement. In all cases, the maximum value of 60% decontamination could be reached at the end of the electrolysis. However, it was already achieved after only ca. 10–15 min at 300 and 200 mA, whereas only 5% TOC removal could be obtained at that time at
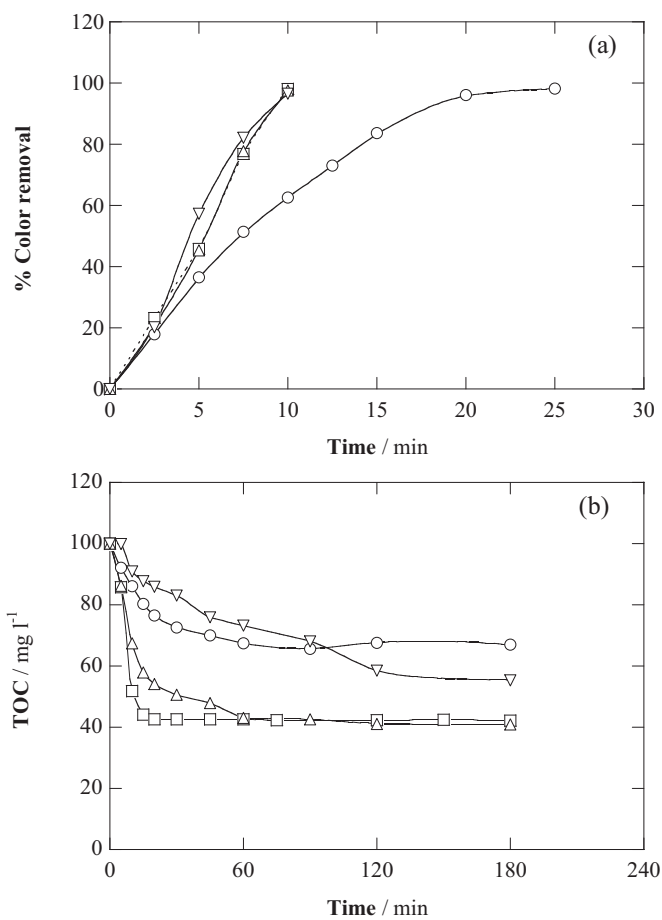
50 and 100 mA. Since overlapping decontamination profiles were observed for 200 and 300 mA, the former current value was considered as optimum for further EC experiments because, despite requiring 15 min instead of 10 min for total decolorization, it entails lower energy consumption. In fact, plots against current charge reveal that a higher current efficiency is obtained at 200 mA (not shown). In conclusion, the best conditions for EC were obtained for the Fe/steel system in 0.05 M NaCl at natural pH 6.3 and 200 mA, which led to complete color removal and maximum TOC abatement in just 15 min.

3.2. Treatment of Tartrazine solutions by electrochemical advanced oxidation processes

The EAOPs have demonstrated their great performance for the treatment of various classes of dyes. This section focuses on the behavior of Tartrazine solutions in different media at pH 3.0 upon application of EO, EF and PEF with steel or ADE as the cathode and Pt or BDD as the anode, at 200 mA. The trends of color removal percentage and TOC abatement are shown in Figs. 5 and 6. The decolorization efficiency in 0.05 M Na$_2$SO$_4$ is depicted in Fig. 5a, revealing a very different performance of EO in comparison to EF and PEF. The color disappeared very slowly in all the EO systems, being required 480 min for total decolorization with BDD and even longer time with Pt. The latter anode only forms low amounts of •OH via reaction (1) and, since it is rather chemisorbed, its oxidation ability is much lower than that of much greater quantities of
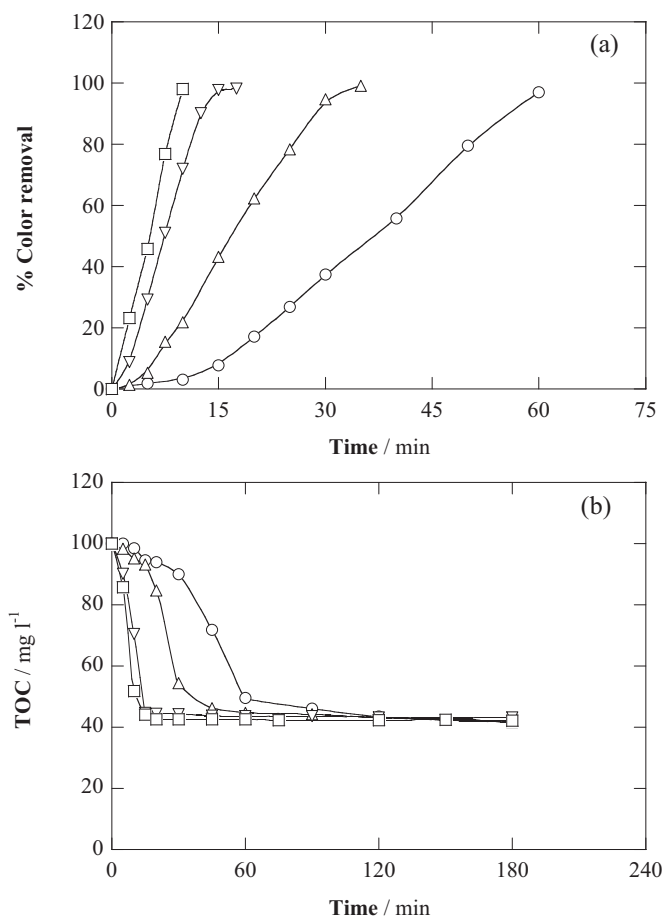
Fig. 4. Effect of current on (a) percentage of color removal at 428 nm and (b) TOC decay with electrolysis time for the EC (Fe/steel) degradation of 130 ml of 278 mg l^{-1} Tartrazine solutions in 0.05 M NaCl at natural (and controlled) pH 6.3 and: (○) 50 mA, (△) 100 mA, (▽) 200 mA and (□) 300 mA.

Fig. 5. (a) Decolorization efficiency and (b) TOC abatement vs electrolysis time for the treatment of 130 ml of 278 mg l^{-1} Tartrazine solutions in 0.05 M Na$_2$SO$_4$ at pH 3.0 and 200 mA by different EAOPs: (●) EO (BDD/ADE), (○) EO (Pt/ADE), (■) EO (BDD/steel), (□) EO (Pt/steel), (▲) EF with BDD, (△) EF with Pt, (♦) PEF with BDD, (◇) PEF with Pt. In EF and PEF, 0.5 mM Fe^{2+} was added to the solution.

physisorbed hydroxyl radicals produced on BDD. In any case, the EO process in batch mode presents serious mass transport limitations whose most immediate consequence is the low degradation rate and large energy consumption. From these curves, it is also clear that other electrogenerated species such as S$_2$O$_8^{2-}$ ions, O$_3$, H$_2$O$_2$ and HO$_2^•$ play a secondary or even negligible oxidation role [5,6]. In contrast, the absorbance at 428 nm decreased very rapidly in the EF and PEF systems. The color was completely removed in 25–30 min, regardless of the anode used and the absence or presence of UVA light. This means that the pre-eminent oxidizing agent in Fenton-based EAOPs in Na$_2$SO$_4$ is $^•$OH formed from Fenton's reaction (9) thanks to the addition of 0.5 mM Fe^{2+} that reacts with cathodically generated H$_2$O$_2$. The fact that reaction (9) occurs in the solution bulk allows overcoming the aforementioned mass transport limitations found in EO. The mineralization ability of all these EAOPs can be seen in Fig. 5b. Here, the lower oxidation power of Pt compared to BDD is much clearer, since 10% and 92% TOC removal was achieved at 480 min by EO with Pt and BDD, respectively. The use of EF cells led to a greater TOC abatement, with 52% TOC decay with Pt and complete mineralization after 300 min with BDD. The extraordinary oxidizing activity of $^•$OH in the bulk is therefore confirmed. The irradiation with UVA lamps in PEF cells led to the quickest mineralization, with all the TOC destroyed after 240 min using either Pt or BDD. Such great performance is due to several concomitant reactions: (i) the photoreduction of Fe(III) (as [Fe(OH)]$^{2+}$) formed in reaction (1), which yields additional $^•$OH and regenerates Fe^{2+} and (ii) the quick photolysis of complexes formed between Fe(III)
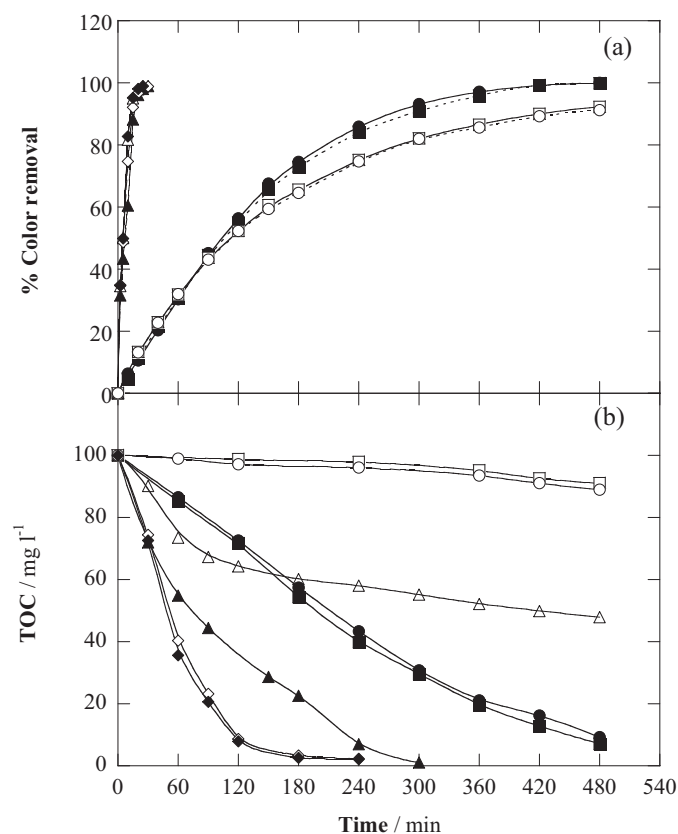
refractory by-products such as short-chain aliphatic carboxylates [5]. Since the nature of the electrolyte was found to have a large influence in EC, the same EAOPs were tested in 0.05 M NaCl. Fig. 6a clearly shows the very positive effect of chloride ions, as shown above for EC. The time for total color removal in the EO systems was reduced from ≥480 min to only 12.5–25 min. EF and PEF, which were already very powerful in Na$_2$SO$_4$, allowed the complete decolorization within a similar time period of only 15–20 min. As can be seen, only a minor enhancement was achieved when changing Pt by BDD. Moreover, the amelioration when using EF and PEF instead of EO with ADE was rather insignificant. It can then be concluded that the presence of active chlorine as the decolorization agent, not confined in the electrodes but dissolved in the whole volume, is essential since it has the preponderant oxidant role over all kinds of $^•$OH formed at the anode surface and in the bulk. Fig. 6b depicts the mineralization curves for the same experiments. The difference with curves in Fig. 6a is straightforward since in this graph the profiles are highly dependent on the cell used. The percentage of TOC removal in EO with Pt was ≥40% at 480 min, which is much higher than that in Na$_2$SO$_4$ due to action of active chlorine species in the bulk. EO with BDD was somewhat better, achieving 88% TOC abatement mainly thanks to the action of $^•$OH formed on BDD that is able to slowly but progressively remove refractory by-products. Note that the TOC decay was a bit slower compared to that in Na$_2$SO$_4$, which can be explained by the parasitic reaction between $^•$OH and Cl$^-$ to form weaker oxidants such as ClOH$^{•-}$, as well as Cl$^•$ and Cl$_2^{•-}$ that can be finally converted into Cl$_2$ [56]. Other wasting reactions between $^•$OH and HClO/ClO$^-$ are also plausible. EF with Pt in NaCl led to 75% TOC removal, which is better than 52% obtained in Na$_2$SO$_4$ due to the action of active chlorine on
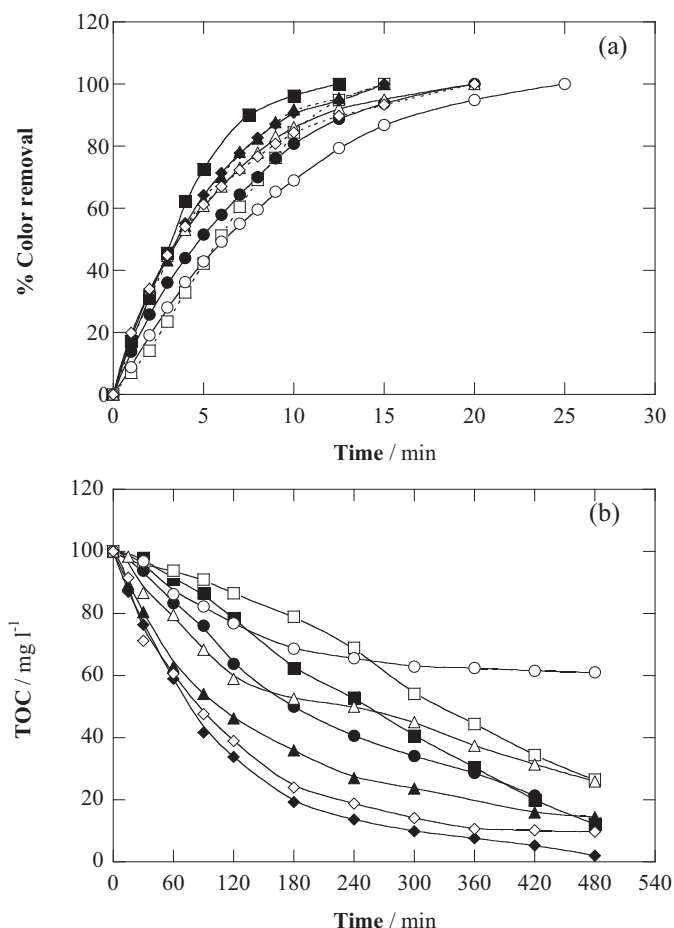
Fig. 7. Active chlorine vs electrolysis time for the PEF (BDD/ADE) degradation of 130 ml of 0.05 M NaCl at pH 3.0 and 200 mA.

in very small quantities, unable to become accumulated but high enough to react with Tartrazine to form chlorinated by-products, as will be later demonstrated. The formation of active chlorine as a bleaching agent during EC of Tartrazine has been hypothesized elsewhere [48].

The aforementioned results confirm the great interest of EAOPs for water treatment. However, the large treatment time required to reach total mineralization is one of their main drawbacks to be implemented as a single degradation step. Therefore, the optimized EC pre-treatment can be envisaged as a powerful solution to make the technology viable and, therefore, appealing to the industry.

3.3. Performance of the coupled EC/EAOPs treatments

Fig. 8 presents the mineralization trends obtained upon the sequential treatment of Tartrazine solutions consisting in an EC step followed by five different EAOPs that had yielded the quickest TOC removal in Fig. 6b. The dye solutions were firstly pre-treated by EC (Fe/steel) in 0.05 M NaCl at natural pH 6.3 and 200 mA for 15 min. This ensured a 100% color removal (Fig. 4a) and 60% TOC abatement, whereupon the TOC content tended to remain unaltered. Then, the samples were centrifuged, and the supernatant was

Fig. 6. Analogous experiments to those shown in Fig. 5 but using solutions with 0.05 M NaCl.

by-products that are refractory to •OH. EF could be enhanced using BDD, reaching 88% TOC abatement, although again the parasitic reactions involving •OH and chlorinated species impedes the complete mineralization in 300 min observed in Na_2SO_4. Finally, the highest performance was achieved again in PEF systems. As happened in EO and EF, reactions between •OH mainly formed on BDD and chlorinated species led to a slower mineralization compared to Na_2SO_4 medium. Therefore, only PEF with BDD allowed the complete mineralization in 480 min, which however was significantly slower than PEF in Na_2SO_4 that yielded the total TOC disappearance in 240 min. In any case, the most remarkable feature is that it is possible to reach the total mineralization by an EAOP in NaCl, which was the optimum electrolyte to carry out the EC treatment.

Hitherto, the decolorization and decontamination profiles in NaCl medium have been explained on the basis of the formation of active chlorine. The existence of such species was then corroborated by electrolyzing solutions of 0.05 M NaCl by PEF with BDD under the previously found optimum conditions. As shown in Fig. 7, active chlorine was accumulated along the electrolysis, which confirms the role of reactions (2)–(4). The accumulated concentration was as low as 4 mg Cl_2 l^{-1}. Independent electrolyses by EO (BDD/steel) showed a much higher concentration at the same time intervals (not shown), which means that the formation of active chlorine is really favored by BDD, despite being partly destroyed by cathodically generated H_2O_2 in PEF [56]. The partial destruction of H_2O_2 in NaCl becomes an additional justification of the worse performance of EF and PEF with BDD explained in Fig. 6b. Solutions of 0.05 M NaCl were also treated by the optimized EC process, but no active chlorine was detected. This means that it is possibly formed
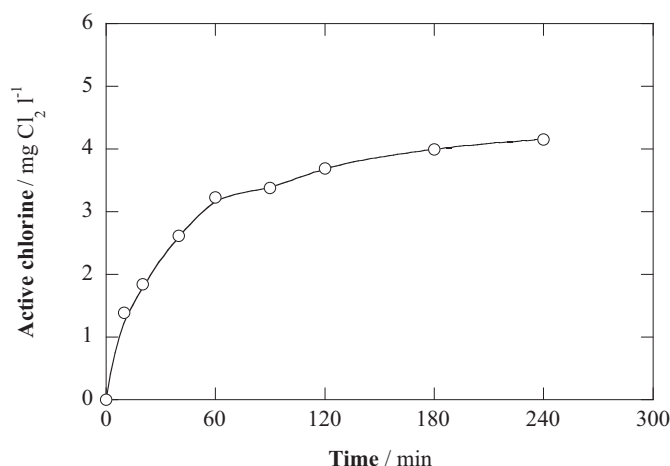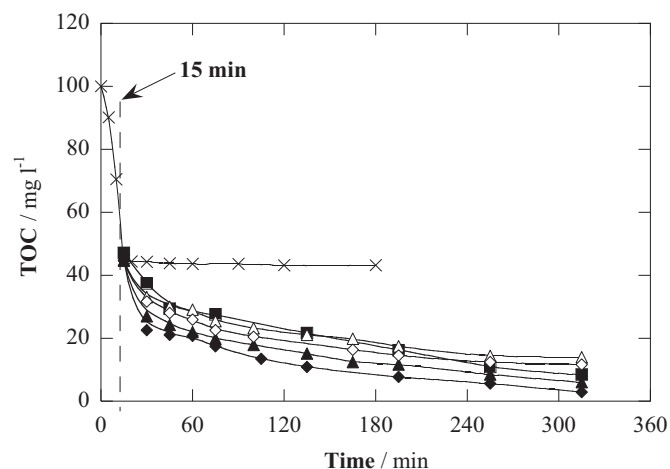

Fig. 8. TOC removal vs electrolysis time for the treatment of 130 ml of 278 mg l^{-1} Tartrazine solutions by various two-step EC (Fe/steel, 15 min, 200 mA, 0.05 M NaCl at natural pH 6.3)/EAOPs (200 mA, pH 3.0): (■) EO (BDD/steel), (△) EF with Pt, (▲) EF with BDD, (◇) PEF with Pt and (♦) PEF with BDD. (×) Comparative TOC removal by EC alone.
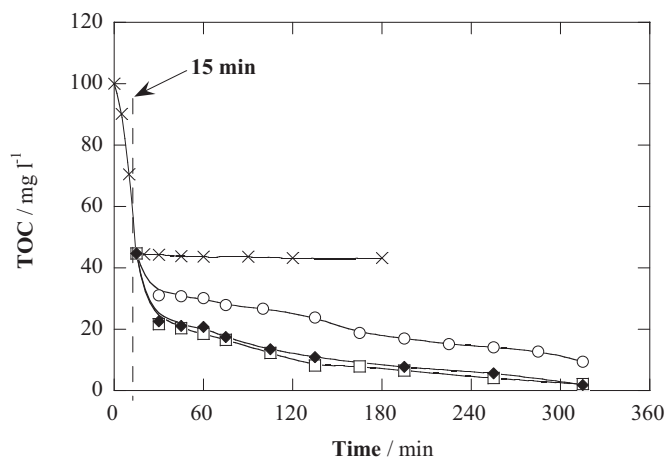
Fig. 9. Effect of current on TOC removal with electrolysis time for the EC/PEF (BDD/ADE) treatment under the conditions shown in Fig. 8 at: (○) 100 mA, (♦) 200 mA and (□) 300 mA.

treated by the EAOPs at 200 mA after pH regulation to 3.0. The total iron concentration after centrifugation and prior to the application of the EAOPs was analyzed, yielding a value of 0.6 mM, which is acceptable because Fenton-based EAOPs with ADE cathodes usually require an iron concentration in the range 0.5–1.0 mM [5]. As can be seen, the five EAOPs allowed the progressive mineralization of the pre-treated solutions. EF and PEF with Pt anode were slightly slower than processes with BDD, reaching 86–88% TOC removal after 315 min (15 min of EC followed by 300 min of EAOP). EO and EF with BDD performed somewhat better due to the additional action of active •OH formed on the anode surface, thus achieving 92 and 95% TOC abatement, respectively. Finally, the PEF (BDD/ADE) treatment of the pre-treated Tartrazine solutions allowed obtaining the fastest decontamination, with total mineralization in about 315 min of global sequential treatment. Coupling of EC with a post-treatment that only consisted in the irradiation of the electrocoagulated solutions with an UVA lamp showed the inefficacy of UVA light alone to remove the TOC. Therefore, the great performance of such PEF as the second step can be explained by the synergistic action of Fe(III) photoreduction, photodecarboxylation of refractory by-products and oxidation of persistent by-products by •OH at BDD and in the bulk, as well as by active chlorine in
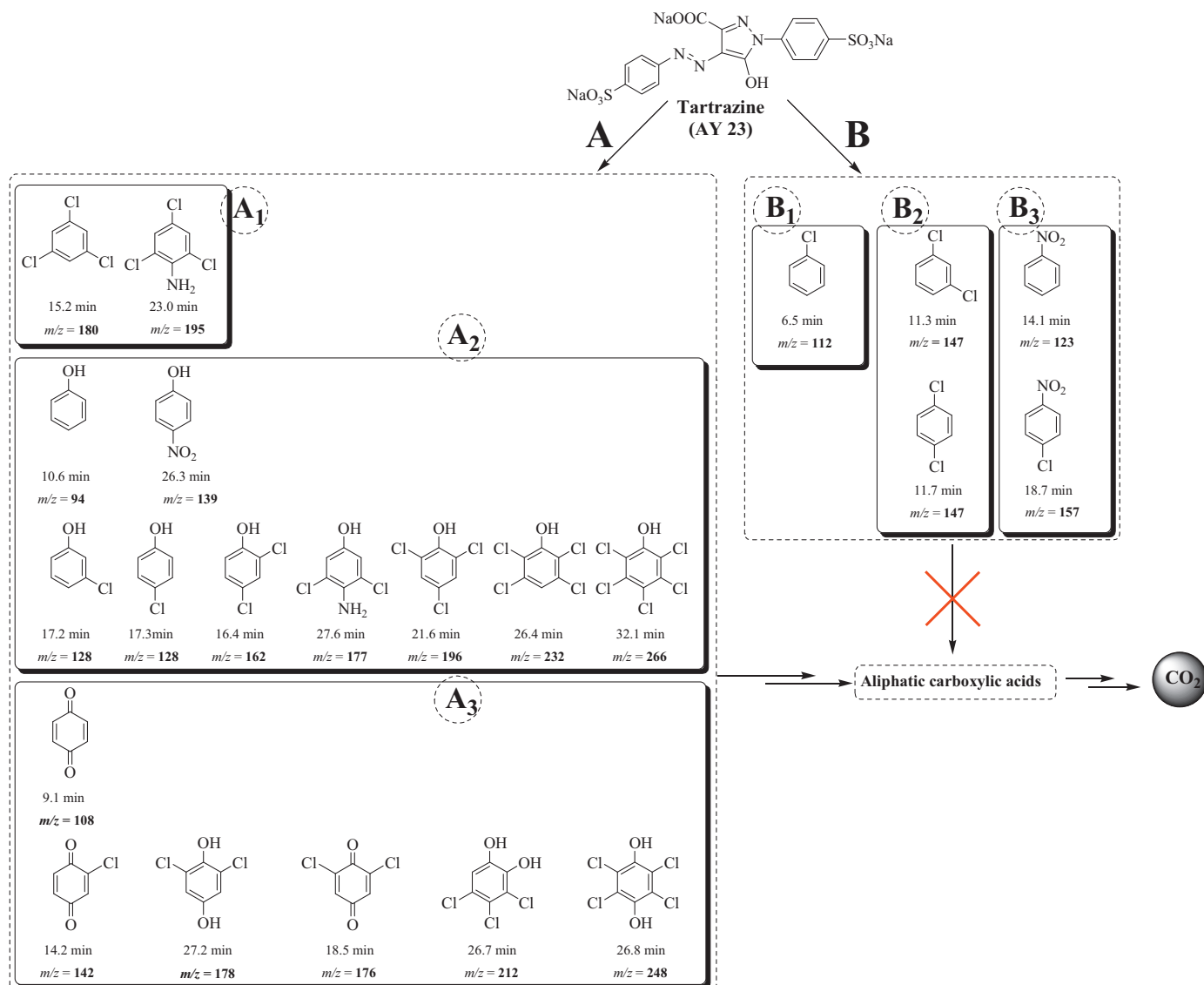

Fig. 10. Reaction by-products identified by GC–MS after: (A) The two-step EC (Fe/steel, 15 min)/PEF (BDD/ADE, 10 min) treatment and (B) EC (Fe/steel, 15 min) alone.

the bulk. The energy consumption per unit volume was calculated for all the sequential treatments according to Eq. (11). The time course of this parameter is not shown because it is simply proportional to the potential difference of each cell, which was around 15 V for cells with Pt and 20–25 V for cells with BDD. Therefore, at 315 min, progressively higher energy consumptions of 110–120, 160 and 190 kW h m^{-3} were required for EF and PEF with Pt, EO with BDD/steel, and EF or PEF with BDD, respectively. The quicker degradation by PEF (BDD/ADE) then had in return a higher energy consumption, which can be lowered by using Pt instead. Obviously, the values are too high due to the use of a small batch cell but, in real-scale applications, with recirculation of larger volumes and employing optimized reactors that allow the decrease of the potential difference, the cost would be dramatically reduced.

The effect of applied current on the mineralization rate obtained by the PEF (BDD/ADE) post-treatment was also studied. Fig. 9 reveals that 200 mA was the optimum value, since it allows a quicker TOC removal compared to 100 mA and an almost identical evolution compared to 300 mA. In conclusion, in the sequential degradation, the EC acted as a very effective coagulation step to quickly decolorize the solutions and, at the same time, as a source of enough iron catalyst for the subsequent EAOPs.

3.4. Identification of Tartrazine degradation by-products

Tartrazine solutions were electrolyzed by using the best EC/PEF treatment under the optimized conditions described in Fig. 8, but stopping the PEF step after 10 min in order to identify the major accumulated aromatic by-products. As shown in pathway A of Fig. 10, up to seventeen compounds could be identified by GC–MS. They can be grouped into three different types: (A$_1$) Non-hydroxylated by-products, which are generated as a result of progressive chlorination of simpler by-products, as well as (A$_2$) monohydroxylated and (A$_3$) dihydroxylated (in the form of phenols and quinones) intermediates formed by the action of •OH at the anode vicinity and in the bulk. Note that A$_2$ and A$_3$ include various polychlorinated hydroxybenzenes (di-, tri-, tetra- and penta-derivatives), which can be explained by the ability of BDD anode to electrogenerate active chlorine, as discussed from Fig. 7. They also include the derivatives 2,4,6-trichlorophenol and 4-amino-3,5-dichlorophenol that come from the hydroxylation of the two products shown in A_1. The scheme of Fig. 10 also informs about the further cleavage of the aryl moiety gathered in path A to yield a mixture of short-chain aliphatic carboxylic acids, with oxalic acid as the main by-product as discussed in our previous works on the electrochemical treatment of benzenic pollutants [5]. As commented from Fig. 8, PEF with BDD allowed the total mineralization of all these by-products to form CO$_2$.

In order to assess the primary decolorization steps undergone by Tartrazine prior to PEF treatment, the mixture of by-products accumulated in the electrocoagulation supernatant under optimized EC conditions for 15 min was analyzed by GC–MS. The pathway B of Fig. 10 includes five by-products such as mono/dichlorobenzene and nitrobenzene derivatives. This indicates the ability of Fe anode to produce active chlorine, as hypothesized above. Since the amount of active chlorine in EC was so small that it could not be identified by spectrophotometric analysis, in contrast to that observed in PEF, a mild chlorination resulted from this pretreatment. Further chlorination and/or hydroxylation of these by-products gave rise to some compounds shown in pathway A upon coupling with PEF. The formation of the five by-products after 15 min in EC, once the azo dye had completely disappeared (Fig. 4a), agrees with the trend of TOC in Fig. 4b showing that ca. 40% of organic matter was still present in the solution. That residual TOC can then be related to such soluble derivatives that cannot be coagulated in EC. Note in the scheme of Fig. 10 that in this case the aryl

moiety cannot be mineralized to aliphatic carboxylic acids, but it is persistent unless a convenient EAOP is coupled.

4. Conclusions

This work results from a collaboration project that aims at envisaging new solutions for the treatment of water effluents contaminated by synthetic dyes. A traditional technology such as EC and some emerging ones like EAOPs including EO, EF and PEF have been firstly investigated individually to assess their ability to decolorize and mineralize solutions of Tartrazine as a model azo dye. The quickest decontamination reported in this communication has been yielded by EC with iron anodes and PEF with H$_2$O$_2$ electrogeneration. It has been demonstrated that the sequential EC (Fe/steel)/PEF (BDD/ADE) treatment favors both, the fast color removal and separation of a large fraction of organic matter by EC, and the destruction of the remaining persistent organic matter in the pre-treated solution by PEF. The complete decolorization and mineralization of solutions were thus achieved within relatively short time periods thanks to coagulation by Fe(OH)$_n$ and oxidation by •OH and active chlorine species. The best conditions involved an EC pre-treatment with Fe/steel in 0.05 M NaCl at natural pH 6.3 and 200 mA for 15 min, followed by centrifugation and treatment of the supernatant by PEF with BDD/ADE at 200 mA and pH 3.0 for ca. 300 min to achieve the complete TOC removal. Up to 17 aromatic by-products were identified by GC–MS during the EC/PEF degradation, which could be totally destroyed in the EAOP step. Therefore, the combined treatment allows overcoming the drawbacks of the single processes, i.e., the only partial mineralization obtained by EC and the long treatment time typically required by EAOPs, thus making the whole electrochemical technology much more cost-effective due to the reduced energy consumption.

References

[1] C. Comninellis, A. Kapalka, S. Malato, S.A. Parsons, I. Poulios, D. Mantzavinos, J. Chem. Technol. Biotechnol. 83 (2008) 769–776.
[2] M. Klavarioti, D. Mantzavinos, D. Kassinos, Environ. Int. 35 (2009) 402–417.
[3] I. Sirés, E. Brillas, Environ. Int. 40 (2012) 212–229.
[4] A. Anglada, A. Urtiaga, I. Ortiz, J. Chem. Technol. Biotechnol. 84 (2009) 1747–1755.
[5] E. Brillas, I. Sirés, M.A. Oturan, Chem. Rev. 109 (2009) 6570–6631.
[6] M. Panizza, G. Cerisola, Chem. Rev. 109 (2009) 6541–6569.
[7] A.M. Polcaro, M. Mascia, S. Palmas, Electrochim. Acta 49 (2004) 649–656.
[8] M. Faouzi, P. Cañizares, A. Gadri, J. Lobato, B. Nasr, R. Paz, M.A. Rodrigo, C. Saez, Electrochim. Acta 52 (2006) 325–331.
[9] E. Butrón, M.E. Juárez, M. Solis, M. Teutli, I. González, J.L. Nava, Electrochim. Acta 52 (2007) 6888–6894.
[10] M. Panizza, A. Kapalka, Ch. Comninellis, Electrochim. Acta 53 (2008) 2289–2295.
[11] M.Y.A. Mollah, R. Schennach, J.R. Parga, D.L. Cocke, J. Hazard. Mater. B84 (2001) 29–41.
[12] S. Zodi, O. Potier, F. Lapicque, J.-P. Leclerc, Desalination 261 (2010) 186–190.
[13] V. Khandegar, A.K. Saroha, J. Environ. Manage. 128 (2013) 949–963.
[14] N. Daneshvar, H.A. Sorkhabi, M.B. Kasiri, J. Hazard. Mater. B112 (2004) 55–62.
[15] A.K. Golder, A.N. Samanta, S. Ray, Sep. Purif. Technol. 53 (2007) 33–41.
[16] H.A. Moreno-Casillas, D.L. Cocke, J.A.G. Gomes, P. Morkovsky, J.R. Parga, E. Peterson, Sep. Purif. Technol. 56 (2007) 204–211.
[17] M. Muthukumar, M.T. Karuppiah, G.B. Raju, Sep. Purif. Technol. 55 (2007) 198–205.
[18] C.A. Martínez-Huitle, E. Brillas, Appl. Catal., B 87 (2009) 105–145.
[19] X.D. Zhang, J.D. Hao, W.S. Li, H.J. Jin, J. Yang, Q.M. Huang, D.S. Lu, H.K. Xu, J. Hazard. Mater. 170 (2009) 883–887.

[20] C.J. Izquierdo, P. Canizares, M.A. Rodrigo, J.P. Leclerc, G. Valentin, F. Lapicque, Desalination 255 (2010) 15–20.

[21] C. Phalakornkule, S. Polgumhang, W. Tongdaung, B. Karakat, T. Nuyut, J. Environ. Manage. 91 (2010) 918–926.

[22] R. Katal, H. Pahlavanzadeh, Desalination 265 (2011) 199–205.

[23] J.M. Peralta-Hernández, Y. Meas-Vong, F.J. Rodríguez, T.W. Chapman, M.I. Maldonado, L.A. Godínez, Water Res. 40 (2006) 1754–1762.

[24] A. Özcan, M.A. Oturan, N. Oturan, Y. Şahin, J. Hazard. Mater. 163 (2009) 1213–1220.

[25] M. Panizza, G. Cerisola, Water Res. 43 (2009) 339–344.

[26] E. Rosales, M. Pazos, M.A. Longo, M.A. Sanromán, Chem. Eng. J. 155 (2009) 62–67.

[27] A. Dirany, I. Sirés, N. Oturan, M.A. Oturan, Chemosphere 81 (2010) 594–602.

[28] N. Oturan, M. Zhou, M.A. Oturan, J. Phys. Chem. A 114 (2010) 10605–10611.

[29] I. Sirés, C.T.J. Low, C. Ponce-de-León, F.C. Walsh, Electrochem. Commun. 12 (2010) 70–74.

[30] E. Isarain-Chávez, C. Arias, P.L. Cabot, F. Centellas, R.M. Rodríguez, J.A. Garrido, E. Brillas, Appl. Catal., B 96 (2010) 361–369.

[31] M.M. Ghoneim, H.S. El-Desoky, N.M. Zidan, Desalination 274 (2011) 22–30.

[32] S. Randazzo, O. Scialdone, E. Brillas, I. Sirés, J. Hazard. Mater. 192 (2011) 1555–1564.

[33] E.J. Ruiz, C. Arias, E. Brillas, A. Hernández-Ramírez, J.M. Peralta-Hernández, Chemosphere 82 (2011) 495–501.

[34] M. Zhou, Q. Tan, Q. Wang, Y. Jiao, N. Oturan, M.A. Oturan, J. Hazard. Mater. 215–216 (2012) 287–293.

[35] S. García-Segura, J.A. Garrido, R.M. Rodríguez, P.L. Cabot, F. Centellas, C. Arias, E. Brillas, Water Res. 46 (2012) 2067–2076.

[36] L. Zhou, Z. Hu, C. Zhang, Z. Bi, T. Jin, M. Zhou, Sep. Purif. Technol. 111 (2013) 131–136.

[37] B. Boye, M.M. Dieng, E. Brillas, Electrochim. Acta 48 (2003) 781–790.

[38] B. Boye, E. Brillas, A. Buso, G. Farnia, C. Flox, M. Giomo, G. Sandonà, Electrochim. Acta 52 (2006) 256–262.

[39] R. Daghrir, P. Drogui, Environ. Chem. Lett. 11 (2013) 151–156.

[40] R.M. Christie (Ed.), Environmental Aspects of Textile Dyeing, Woodhead Publ. Ltd., Cambridge, England, 2007.

[41] S. Chapman, Food Standards Agency, Report Number FMT/21810/1, Campden Technol. Ltd., 2011 March.

[42] EFSA Panel on Dietetic Products, Nutrition and Allergies (NDA), EFSA Journal 8 (2010) 1778-1788.

[43] D. Rajkumar, B.J. Song, J.G. Kim, Dyes Pigm. 72 (2007) 1–7.

[44] A. Sakalis, D. Vaněrková, M. Holčapek, P. Jandera, A. Voulgaropoulos, Chemosphere 67 (2007) 1940–1948.

[45] M. Zhou, Q. Yu, L. Lei, G. Barton, Sep. Purif. Technol. 57 (2007) 380–387.

[46] M. Zhou, Q. Yu, L. Lei, Dyes Pigm. 77 (2008) 129–136.

[47] N. Daneshvar, A.R. Khataee, A.R.A. Ghadim, M.H. Rasoulifard, J. Hazard. Mater. 148 (2007) 566–572.

[48] N. Modirshahla, M.A. Behnajady, S. Kooshaiian, Dyes Pigm. 74 (2007) 249–257.

[49] G.B. Raju, M.T. Karuppiah, S.S. Latha, S. Parvathy, S. Prabhakar, Chem. Eng. J. 144 (2008) 51–58.

[50] M. Panizza, G. Cerisola, J. Electroanal. Chem. 638 (2010) 236–240.

[51] S. Cotillas, J. Llanos, P. Cañizares, S. Mateo, M.A. Rodrigo, Water Res. 47 (2013) 1741–1750.

[52] APWA, AWWA, WEF, Standard methods for the examination of water and wastewater, in: Method number 4500-Cl Chlorine (residual)—G. DPD Colorimetric Method, 21st ed., American Public Health Association, Washington, DC, 2005, pp. 4–67 to 4–68.

[53] N.H. Furman (Ed.), Standard Methods of Chemical Analysis, 1, sixth ed., R.E. Krieger Pub. Co, Huntington, NY, 1975, p. 553.

[54] O.J. Flores, J.L. Nava, G. Carreño, E. Elorza, F. Martínez, Chem. Eng. Sci. 97 (2013) 1–6.

[55] Y.Ş. Yildiz, A.S. Koparal, Ş. Írdemez, B. Keskinler, J. Hazard. Mater. B139 (2007) 373–380.

[56] J. De Laat, G.T. Le, B. Legube, Chemosphere 55 (2004) 715–723.